

An application of distributed approximating functional-wavelets to reactive scattering

G. W. Wei, S. C. Althorpe, and D. J. Kouri

Department of Chemistry and Department of Physics, University of Houston, Houston, Texas 77204-5641

D. K. Hoffman

Department of Chemistry and Ames Laboratory, Iowa State University, Ames, Iowa 50011

(Received 6 October 1997; accepted 9 January 1998)

A newly developed distributed approximating functional (DAF)-wavelet, the Dirichlet-Gabor DAF-wavelet (DGDW), is applied in a calculation of the state-to-state reaction probabilities for the three-dimensional (3-D) ($J=0$)H+H₂ reaction, using the time-independent wave-packet reactant-product decoupling (TIWRPD) method. The DGDWs are reconstructed from a rigorous mathematical sampling theorem, and are shown to be DAF-wavelet generalizations of both the sine discrete variable representation (sinc-DVR) and the Fourier distributed approximating functionals (DAFs). An important feature of the generalized sinc-DVR representation is that the grid points are distributed at equally spaced intervals and the kinetic energy matrix has a banded, Toeplitz structure. Test calculations show that, in accordance with mathematical sampling theory, the DAF-windowed sinc-DVR converges much more rapidly and to higher accuracy with bandwidth, $2W+1$. The results of the H+H₂ calculation are in very close agreement with the results of previous TIWRPD calculations, demonstrating that the DGDW representation is an accurate and efficient representation for use in FFT wave-packet propagation methods, and that, more generally, the theory of wavelets and related techniques have great potential for the study of molecular dynamics.

© 1998 American Institute of Physics. [S0021-9606(98)02114-X]

I. INTRODUCTION

By exploiting recent advances in molecular-beam technology, experimentalists are now able to study elementary chemical processes (in such areas as reactive scattering, photodissociation, and gas-surface scattering) at an unprecedented level of detail, measuring state-resolved product distributions, cross sections, and vector correlations for a wide range of polyatomic systems. In seeking to interpret this data, theoreticians have developed new methods of solving the Schrodinger equation for nuclear dynamics, many of which rely on efficient representations of the (multidimensional) Hamiltonian. Probably the most important theoretical advances in this regard have been the discrete grid representations, with the most widely used being the discrete variable representation (DVR).¹

The DVR is a spectral method, which provides a global representation of the (exact) wave function at each grid point. It becomes especially powerful when combined with the fast Fourier transform (FFT) algorithm in wave-packet propagation methods. When applying the latter, an equally spaced grid of points is distributed along each coordinate, enabling the propagator to be converted easily between coordinate space and momentum space. The calculation then scales as only $N \log N$. It is this efficiency, along with many other important techniques, that has recently enabled the Schrodinger equation to be solved, in the body frame, for four atom reactive scattering. This involves solving coupled partial differential equations in six relative degrees of freedom. However, the global nature in most spectral methods may limit their application to even larger scale computations.

For example, if one uses an average of ten basis functions per degree of freedom, a five-atom system will require a Hamiltonian matrix of dimension $10^9 \times 10^9$, compared to $10^6 \times 10^6$ for a four-atom system. Therefore any reduction in matrix size will undoubtedly be important for the further development of the field. One possible reduction can be achieved through changing the full Hamiltonian matrix into a sparse matrix. This means replacing the global basis function expansion with a banded, local spectral method which has global method accuracy and local method bandness. Being intimately related to the theory of approximations, and minimum support bases, wavelet theory has been expected to fulfill this task and has been extensively studied recently for this purpose.²⁻⁷ However, these efforts have been hindered either by the technical difficulties of incorporating the treatment of boundary conditions into a multiresolution analysis framework, or by the lack of accurate and efficient wavelets or wavelet packets for solving partial differential equations (PDEs). In this paper, we employ a recently developed distributed approximating functional (DAF)-wavelet, the Dirichlet-Gabor DAF-wavelet⁸ (DGDW), to obtain a discrete grid representation of the Hamiltonian for use in FFT wave-packet propagation methods. Our wavelet method has been obtained as a wavelet extension of our previous distributed approximating functionals,⁹ but it can also be viewed as a generalization (regularization) of the sinc-DVR method.

The subject of wavelet analysis has recently drawn a great deal of attention from mathematical scientists in various disciplines. It is still in the midst of an important growth stage during which theory and practical applications are be-

ing compared with existing methods. Among these applications, wavelets have been used most widely for data compression and signal processing. They have become a tool for analyzing fractals and iterative schemes associated with dynamical systems. Signal processing methods such as quadrature mirror filters go hand in hand with wavelet techniques for studying a host of communications problems. The fundamental aspects of classical turbulence are also being studied using wavelet packets, and there have been applications of wavelet theory in theoretical physics, oil exploration, irregular sampling, and singular integral operators. The present work suggests that wavelet methods can also play an important role in quantum scattering computations.

II. THEORY

The DGDW is defined as⁸

$$\begin{aligned}\phi(x) &= C_{M,\sigma} e^{-x^2/2\sigma^2} \left[\frac{1}{2} + \sum_{k=1}^M \cos(kx) \right] \\ &= C_{M,\sigma} e^{-x^2/2\sigma^2} \left[\frac{\sin(M + \frac{1}{2})x}{2 \sin x/2} \right],\end{aligned}\quad (1)$$

where the constant $C_{M\sigma}$ is determined by the Fourier transform $\hat{\phi}$ of ϕ :

$$\begin{aligned}\hat{\phi}(0) &= \int \phi(x) dx \\ &= C_{M\sigma} \sqrt{2\pi\sigma} \left[\frac{1}{2} + \sum_{k=1}^M \exp\left(-\frac{\sigma^2 k^2}{2}\right) \right] = 1.\end{aligned}\quad (2)$$

(This property is characteristic of a ‘‘father wavelet’’.¹⁰) The DGDW has been constructed by combining Gabor wavelets,^{11,12} defined by

$$G_{a_k,\sigma}(x) = e^{-x^2/2\sigma^2} \cos(a_k x),\quad (3)$$

with the Dirichlet kernel

$$D_M(x) = \frac{1}{\pi} \left[\frac{1}{2} + \sum_{k=1}^M \cos(kx) \right] = \frac{\sin(M + \frac{1}{2})x}{2\pi \sin x/2}.\quad (4)$$

The Dirichlet kernel can be regarded as a discrete orthogonal Fourier basis function expansion of the Dirac delta function

$$\lim_{M \rightarrow \infty} D_M(x - x') = \delta(x - x'),\quad (5)$$

and therefore it coincides with our discrete Fourier DAF.⁹ The DGDWs are, in fact, generalized delta sequences. Thus it is seen that for a given finite σ ,

$$\lim_{M \rightarrow \infty} (C_{M,\sigma} \pi)^{-1} \phi(x) = e^{-x^2/2\sigma^2} \delta(x)\quad (6)$$

is effectively a delta function. Furthermore, when σ approaches zero,

$$\begin{aligned}\lim_{\sigma \rightarrow 0^+} \left\{ C_{M,\sigma} \sqrt{2\pi\sigma} \left(M + \frac{1}{2} \right) \right\}^{-1} \phi(x) \\ = \left[\frac{\sin(M + \frac{1}{2})x}{(2M + 1) \sin x/2} \right] \delta(x),\end{aligned}\quad (7)$$

is also effectively a delta function because the quantity in square brackets is unity in the presence of $\delta(x)$. Hence DGDWs are generalized DAFs. We use the word ‘‘generalized’’ because, from a mathematical point of view, there is an important difference between the discrete Fourier DAF, Eq. (4), and our DGDWs: the former is based on the classical theory of orthogonal basis set expansions, whereas the latter is a nonorthogonal function representation. Such a representation belongs to a new branch of mathematics, the theory of frames.¹³ Formally, both a basis and a frame provide a complete description of an L^2 space (if that is what one is interested in), because nonorthogonal functions in a frame can always be orthonormalized by standard techniques. Thus a frame can be equivalent to a basis since both are complete. However, important differences arise whenever the completeness is not fulfilled.

Our DGDW can be rederived in an alternative fashion. One can start from a mathematical sampling theorem for a function $f(x)$ which satisfies the Dirichlet boundary condition, is periodic in T , and bandlimited to the highest (radial) frequency $2\pi M/T$. In such a case, $f(x)$ can be completely reconstructed from a finite $(2M + 1)$ set of discrete sampling (grid) points¹⁴

$$f(x) = \sum_{k=-M}^M f(x_k) \frac{\sin[\pi/\Delta(x - x_k)]}{(2M + 1) \sin[\pi/T(x - x_k)]},\quad (8)$$

where $\Delta = T/(2M + 1)$ is the sampling interval (grid spacing) and the $x_k = k\Delta$ are the sampling points. Using earlier arguments about the contradiction between bandlimited functions and the physical world,^{15,16} we then construct the following approximate sampling formula

$$\begin{aligned}f(x) \approx \sum_{k=-W}^W f(x_k) \frac{\sin[\pi/\Delta(x - x_k)]}{(2M + 1) \sin[\pi/T(x - x_k)]} \\ \times e^{-(x - x_k)^2/2\sigma^2},\end{aligned}\quad (9)$$

where W , the computational bandwidth, is smaller than M . The sampling (grid) points $\{x_k\}$ are distributed around the point of interest x . Obviously when σ approaches zero we still have a Dirac delta function, as we have shown in Eq. (7). But, setting $W = M$, when $\sigma \rightarrow \infty$, we recover the exact sampling theorem Eq. (8). It is also interesting to examine the limit of M with a fixed Δ :

$$\begin{aligned}\lim_{M \rightarrow \infty} \frac{\sin[\pi/\Delta(x - x_k)]}{(2M + 1) \sin[\pi/T(x - x_k)]} e^{(x - x_k)^2/2\sigma^2} \\ = \frac{\sin[\pi/\Delta(x - x_k)]}{\pi/\Delta(x - x_k)} e^{-(x - x_k)^2/2\sigma^2}.\end{aligned}\quad (10)$$

We call $\sin[\pi/\Delta(x - x_k)]/[\pi/\Delta(x - x_k)] e^{-(x - x_k)^2/2\sigma^2}$ the Shannon–Gabor DAF-wavelet¹⁶ (SGDW), which is a special case of our previous Lagrange DAF.^{17,15} Both the DGDW

TABLE I. L_∞ errors of sinc-DVR and SGDW samplings for predicting functions off a grid and their 1st and 2nd derivatives on the grid of a fixed spacing ($\Delta = \pi/29$). The errors are calculated in the interval of $[0, \pi]$ using various sampling bandwidths, $(2W + 1)$. The σ/Δ parameter used for the SGDW is 3.5.

W	$f_1(x) = \cos x \sin 4x$						$f_2(x) = e^{-x^2/120} \cos x \sin 4x$					
	sinc-DVR			SGDW			sinc-DVR			SGDW		
	f_1	$f_1^{(1)}$	$f_1^{(2)}$	f_1	$f_1^{(1)}$	$f_1^{(2)}$	f_2	$f_2^{(1)}$	$f_2^{(2)}$	f_2	$f_2^{(1)}$	$f_2^{(2)}$
2	3.94(-2)	1.71(-0)	1.10(+1)	1.98(-2)	1.22(-0)	1.32(+1)	3.89(-2)	1.70(-0)	1.10(+1)	1.98(-2)	1.22(-0)	1.32(+1)
4	2.61(-2)	9.55(-1)	3.26(-0)	5.51(-3)	3.49(-1)	3.83(-0)	2.56(-2)	9.41(-1)	3.26(-0)	5.49(-3)	3.48(-1)	3.82(-0)
8	6.74(-3)	2.21(-1)	3.75(-1)	1.26(-4)	9.51(-3)	1.44(-1)	6.52(-3)	2.14(-1)	3.75(-1)	1.25(-4)	9.44(-3)	1.43(-1)
16	2.02(-3)	6.18(-2)	4.48(-2)	5.88(-9)	6.96(-7)	1.83(-5)	1.87(-3)	5.77(-2)	4.47(-2)	5.72(-9)	6.77(-7)	1.78(-5)
32	6.97(-3)	2.06(-1)	5.53(-2)	7.77(-16)	3.55(-15)	6.22(-14)	5.76(-3)	1.71(-1)	5.43(-2)	8.88(-16)	1.78(-15)	6.22(-14)
64	9.97(-4)	2.91(-2)	2.56(-3)	7.77(-16)	3.55(-15)	6.22(-14)	5.60(-4)	1.64(-2)	2.26(-3)	8.88(-16)	1.78(-15)	6.22(-14)
128	3.59(-4)	1.04(-2)	2.75(-4)	7.77(-16)	3.55(-15)	6.22(-14)	5.30(-5)	1.55(-3)	1.14(-4)	8.88(-16)	1.78(-15)	6.22(-14)
256	9.88(-4)	2.87(-2)	2.10(-4)	7.77(-16)	3.55(-15)	6.22(-14)	9.96(-7)	2.90(-5)	1.45(-6)	8.88(-16)	1.78(-15)	6.22(-14)
512	2.68(-4)	7.77(-3)	1.50(-5)	7.77(-16)	3.55(-15)	6.22(-14)	3.00(-15)	3.38(-14)	4.57(-13)	8.88(-16)	1.78(-15)	6.22(-14)
1024	1.36(-4)	3.94(-3)	1.96(-6)	7.77(-16)	3.55(-15)	6.22(-14)	1.89(-15)	5.33(-15)	4.28(-13)	8.88(-16)	1.78(-15)	6.22(-14)

and the SGDW are generalizations of the (infinite grid) sinc-DVR,^{1,18} $\sin[\pi/\Delta(x-x_k)]/[\pi/\Delta(x-x_k)]$ (which is also the continuous Fourier DAF on a grid⁹), as the DGDW reduces to the sinc-DVR in the simultaneous limits of $M \rightarrow \infty$ (with fixed Δ) and $\sigma \rightarrow \infty$, and the SGDW reduces to the sinc-DVR in the limit of $\sigma \rightarrow \infty$:

$$\begin{aligned} \lim_{M \rightarrow \infty, \sigma \rightarrow \infty} \frac{\sin[\pi/\Delta(x-x_k)]}{(2M+1)\sin[\pi/T(x-x_k)]} e^{-(x-x_k)^2/2\sigma^2} \\ = \lim_{\sigma \rightarrow \infty} \frac{\sin[\pi/\Delta(x-x_k)]}{\pi/\Delta(x-x_k)} e^{-(x-x_k)^2/2\sigma^2} \\ = \frac{\sin[\pi/\Delta(x-x_k)]}{\pi/\Delta(x-x_k)}. \end{aligned} \tag{11}$$

In this sense, our DGDW and SGDW can be regarded as a DAF-windowed sinc-DVR or a regularized sinc-DVR. Window functions and regularization are important mathematical topics and they have wide applications in science and engineering. Due to the Gabor or DAF window, the regularized sinc-DVR matrix is highly banded in both physical and Fourier spaces. This endows the regularized sinc-DVRs with great potential for applications in large scale computations.

III. TEST CALCULATIONS

The same considerations governing discrete sampling and the ability to reconstruct a function that forms the basis of signal processing also apply to discretization of partial differential operators. One of the basic theorems is Shannon’s sampling theorem,¹⁹ which states that provided the spacing between grid points is less than a particular value (determined by a maximum frequency or wave number contained in the function of interest), for functions which are “bandlimited” (i.e., that are nonzero only in a finite interval in the frequency or wave-number space), the function can be exactly reproduced provided one samples on the entire real axis. This implies that all derivatives of such a function are also exactly reproduced. The kernel for Shannon’s sampling is, in fact, exactly given by the sinc-DVR. Thus provided the function of interest is bandlimited, the sinc-DVR (summed over infinitely many uniform, discrete grid points) will be

exact. However, if the sampling is truncated to a finite number of grid points, the sinc-DVR is no longer exact, and in fact, one will observe “Gibbs’ oscillations” in the sinc-DVR approximation to a bandlimited function. The presence of these oscillations is related to the lack of smoothness of the sinc-DVR in Fourier space. In general, the controlling factors in optimizing sampling is for the “sampling window” to be as smooth as possible and as compact as possible in both “time” and “frequency” domains. This can greatly reduce the number of sampling points needed to obtain a given level of accuracy, which in turn makes the bandwidth of the sampling matrix as small as possible. In Table I we compare the sinc-DVR and SGDW sampling for reproducing several functions, and their first and second derivatives, with finite numbers of grid sampling points (W) on either side of the point being predicted. The first function, $f_1(x) = \cos x \sin 4x$, is bandlimited and has the general behavior of a scattering wave function in the time-independent close coupling approach. The second function, $f_2(x) = e^{-x^2/120}[\cos x \sin 4x]$, has a Gaussian envelope multiplied into the first function. Thus $f_2(x)$ is not bandlimited, is L^2 , and behaves like a wave-packet state. The maximum or L_∞ errors for W -sampling points on each side of the various grid points are given. We see that for $f_1(x)$, when $W=8$, the SGDW sampling is significantly more accurate than the sinc-DVR, and by $W=32$, the SGDW has attained machine-level accuracy. Even with $W=1024$, the sinc-DVR cannot obtain such high accuracy. This is a reflection of the noncompact nature of the function (i.e., that it does not go to zero for large $|x|$). However, the SGDW has no difficulty in capturing the function with a reasonable bandwidth. The wave-packet-like $f_2(x)$ is easier for the sinc-DVR to deal with. However, again, for $W=8$, the SGDW is significantly more accurate, and already for $W=32$, the SGDW achieves machine-level accuracy. The result is that the SGDW delivers much higher accuracy with smaller W than is possible with the sinc-DVR. We note that no attempt to optimize the SGDW parameters was made. If one used $\sigma=3.0\Delta$, the SGDW results at W values smaller than 32 would be even more accurate. The sinc-DVR does not have an analogous “tuning parameter.”

In the remainder of this section we demonstrate that the

DGDWs may be used as an efficient discrete grid representation of the Hamiltonian in wave-packet propagation methods. In the DGDW representation, the potential energy part of the Hamiltonian is diagonal (as it is in the DVR and other DAF representations); the kinetic energy part is constructed from the second derivative matrix,⁹

$$\delta^{(2)}(x_i - x_k) = \left[\frac{\sin[\pi/\Delta(x - x_k)]}{(2M + 1)\sin[\pi/T(x - x_k)]} \right]_{x=x_i}^{(2)} \times e^{-(x-x_k)^2/2\sigma^2} \quad (12)$$

In the calculations described below we choose $M=35$, $W=32$, and $\sigma/\Delta=3.173$.

For our example calculation, we compute the state-to-state reaction probabilities for the three-dimensional ($J=0$) $\text{H}+\text{H}_2$ reaction, by means of the time-independent wave-packet (TIW) reactant-product decoupling (RPD) method.^{20–24} The latter is a new method for calculating the (exact) state-to-state reaction probabilities which derives from Peng and Zhang's time-dependent RPD formulation of reactive scattering. The wave packet is first propagated in the reactant arrangement of the reaction, which is the region of coordinate space obtained by blocking off all the product arrangements with absorbing potentials (called ‘partitioning-potentials’). The absorbed parts of the wave packet are then reemitted as source terms, each of which is propagated (in a completely separate calculation) down the appropriate product channel. The propagations are evaluated using an extended version of the familiar Chebyshev propagator.

Many aspects of the calculation are the same as in our previous TIWRPD calculation for the 3-D ($J=0$) $\text{H}+\text{H}_2$ reactions, to which the reader is referred for more details. We represent the Hamiltonian in (nonmass weighted) 3-D Jacobi coordinates (R, r, θ) (defined according to the usual convention) which are aligned with respect to either the reactant or the product arrangement of the reaction. Each of the radial coordinates is represented in the DGDW representation, with the exception of the product-arrangement r coordinate, which can be represented very efficiently in terms of the H_2 vibrational DVR. The angle θ is represented in the Gauss–Legendre DVR.

The DGDW representations were constructed using the same evenly spaced grid as that used for the corresponding Hermite DAF representations in Refs. 21 and 22. We evaluated the action of the DGDW kinetic energy operators efficiently by means of the (standard) FFT convolution algorithm,^{25,26} just as was done with DAFs. An important step in solving the TIWRPD equations is the fitting of a set of source terms [located in the region of the partitioning potential(s)] from reactant-arrangement to product-arrangement coordinates. In performing this fitting, we used the DGDW approximation to the Dirac delta function in the same way that we used the Hermite DAF approximation in Refs. 21 and 22. The results of the 3-D DGDW calculation are shown in Figs. 1 and 2, where they are compared with the results of our previous TIWRPD calculation (in which

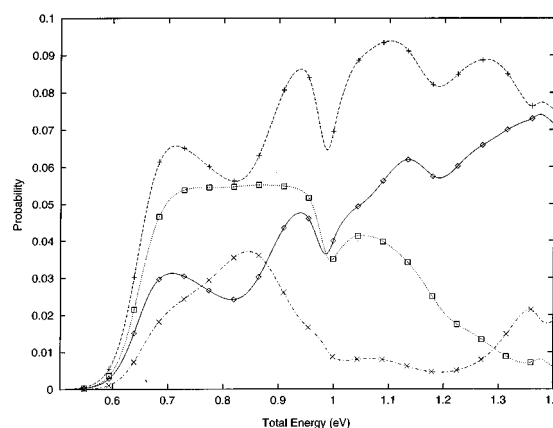


FIG. 1. State-to-state reaction probabilities $R(\nu_0=0, j_0=0 \rightarrow \nu=0, j)$ calculated for the 3-D ($J=0$) $\text{H}+\text{H}_2$ reaction for $j=0$ (solid line), $j=1$ (dashed line), $j=2$ (dotted line), and $j=3$ (chained line). The curves are the results of solving the TIWRPD equations using the DGDW representation. The points (taken from Ref. 22) are the results of solving the TIWRPD equations using the Hermite DAF representation.

we used the Gauss–Hermite DAF representation). The two sets of results are clearly in very close agreement.

Both the DGDW and the Hermite DAF provide banded matrix representations of the Schrödinger operator and are robust and flexible for not only the linear PDEs but also for various nonlinear PDEs with complex geometries and boundary conditions. However, the DGDW is easier to use in solving PDEs because for a given M there are a wider range of σ/Δ values which can be chosen. The common mathematical foundation for both methods is the theory of distributions. A unified description of the DGDW, the Hermite DAF, and wavelets will be given elsewhere.

IV. CONCLUSION

We have demonstrated that DGDWs are the wavelet generalizations of the sinc-DVR and of the (discrete and continuous) Fourier DAFs. They reduce to the familiar DVR method and Fourier DAFs at the appropriate limits. We have also rederived the DGDWs from a rigorous mathematical sampling theorem. The robustness of our approach has been demonstrated by comparing the sampling bandwidth, $2W$

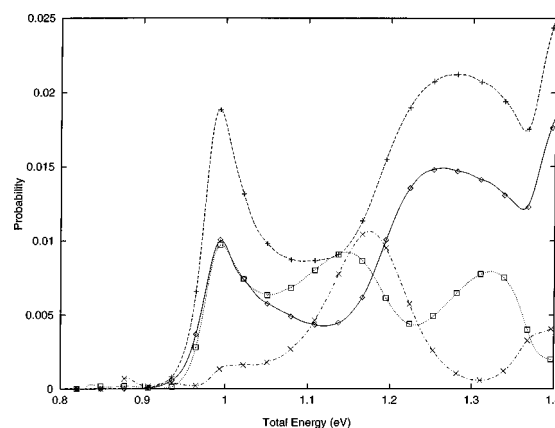


FIG. 2. Same as Fig. 1 for $R(\nu_0=0, j_0=0 \rightarrow \nu=1, j)$.

+1, required by the SGDW and the familiar sinc-DVR in order to fit, to high accuracy, two functions, along with their first and second derivatives. The functions are qualitatively of the form of a close coupling radial wave function and a wave packet. In our application to reactive scattering, we have illustrated how the DGDW can be used to construct a discrete grid representation of the Hamiltonian, in which the grid points are distributed at equally spaced intervals. The DGDW representation of the kinetic energy matrix (like the sinc-DVR) then has a banded, Toeplitz structure, which can be evaluated efficiently by means of the standard FFT convolution algorithm. Our results show that the DGDW representation is an accurate and efficient representation for use in wave-packet propagation (and related) methods, and that, more generally, the theory of wavelets and related techniques have great potential for the study of molecular dynamics.

ACKNOWLEDGMENTS

G.W.W. is supported under an NSERC postdoctoral fellowship and also under R. A. Welch Foundation Grant No. E-0608. S.C.A. is supported under National Science Foundation Grant No. CHE-9700297. D.J.K. is supported in part under R. A. Welch Foundation Grant No. E-0608. Partial support from the Petroleum Research Fund, administered by the American Chemical Society, is also acknowledged. The Ames Laboratory is operated for the Department of Energy by Iowa State University under Contract No. 2-7405-ENG82.

- ¹J. V. Lill, G. A. Parker, and J. C. Light, *Chem. Phys. Lett.* **89**, 483 (1982); J. C. Light, J. P. Hamilton, and J. V. Lill, *ibid.* **82**, 1400 (1985).
²G. Beylkin and J. M. Keiser, *J. Comput. Phys.* **132**, 233 (1997).
³J. Fröhlich and K. Schneider, *J. Comput. Phys.* **130**, 174 (1997).
⁴W. K. Liu and Y. Chen, *Int. J. Numer. Methods Fluids* **21**, 901 (1995).

- ⁵B. Jawerth and W. Swelden, *SIAM (Soc. Ind. Appl. Math.) Rev.* **36**, 377 (1994).
⁶W. Dahmen and A. Kunoth, *Numer. Math.* **63**, 315 (1992).
⁷R. L. Schult and H. W. Wyld, *Phys. Rev. A* **46**, 12 (1992).
⁸G. W. Wei, D. S. Zhang, D. J. Kouri, and D. K. Hoffman, *Phys. Rev. Lett.* **79**, 775 (1997).
⁹D. K. Hoffman, N. Nayar, O. A. Sharafeddin, and D. J. Kouri, *J. Phys. Chem.* **95**, 8299 (1991).
¹⁰C. K. Chui, *An Introduction to Wavelets* (Academic, San Diego, 1992).
¹¹D. Casasent and R. Shenoy, in *Wavelet Applications II*, SPIE Proceedings, edited by H. H. Szu (IEEE Signal Processing Society, Orlando, 1995); in *Wavelet Applications III*, SPIE Proceedings, edited by H. H. Szu (IEEE Signal Processing Society, Orlando, 1996).
¹²F. Bergeaud and S. Mallat, in *Wavelet Applications II*, SPIE Proceedings, edited by H. H. Szu (IEEE Signal Processing Society, Orlando, 1995).
¹³K. Gerald, *A Friendly Guide to Wavelets* (Birkhäuser, Boston, 1994).
¹⁴H. Stark, *J. Opt. Soc. Am.* **69**, 1519 (1979).
¹⁵G. W. Wei, S. C. Althorpe, D. J. Kouri, and D. K. Hoffman, *Phys. Rev. A* (to be published).
¹⁶D. K. Hoffman, G. W. Wei, and D. J. Kouri, *Chem. Phys. Lett.* (to be published).
¹⁷G. W. Wei, D. S. Zhang, D. J. Kouri, and D. K. Hoffman, *Phys. Rev. Lett.* **79**, 775 (1997).
¹⁸D. T. Colbert and W. H. Miller, *J. Chem. Phys.* **96**, 1982 (1991).
¹⁹C. E. Shannon, A mathematical theory of communication, *Bell Syst. Tech. J.* **27**, 379 (1948).
²⁰S. C. Althorpe, D. J. Kouri, D. K. Hoffman, and J. Z. H. Zhang, *J. Chem. Soc., Faraday Trans.* **93**, 703 (1997).
²¹S. C. Althorpe, D. J. Kouri, and D. K. Hoffman, *J. Chem. Phys.* **106**, 7629 (1997).
²²S. C. Althorpe, D. J. Kouri, and D. K. Hoffman, *Chem. Phys. Lett.* **275**, 173 (1997).
²³S. C. Althorpe, D. J. Kouri, and D. K. Hoffman, *J. Chem. Phys.* **107**, 7816 (1997).
²⁴T. Peng and J. Z. H. Zhang, *J. Chem. Phys.* **105**, 6072 (1996); W. Zhu, T. Peng, and J. Z. H. Zhang, *J. Chem. Phys.* **106**, 1742 (1997).
²⁵H. J. Nussbaumer, *Fast Fourier Transform and Convolution Algorithms* (Springer-Verlag, New York, 1982).
²⁶W. H. Press, B. P. Flannery, S. A. Teukolsky, and W. T. Vetterling, *Numerical Recipes* (Cambridge University Press, Cambridge, England, 1986).